ISBN: 978-3-95450-227-1 ISSN: 2673-5490 doi:10.18429/JACoW-IPAC2022-THPOMS010

HEATING AND BEAM IMPACT OF HIGH INTENSITY EXIT WINDOWS FOR FLASHLAB@PITZ

Z. Amirkhanyan[†,1], M. Schmitz[2], Z. Aboulbanine[3], X. Li, H. Qian, M. Gross, M. Krasilnikov, A. Oppelt, R. Niemczyk, S. Philipp, T. Kuhl, F. Stephan, DESY Zeuthen, Germany
[1]on leave from CANDLE Synchrotron Research Institute, Yerevan, Armenia
[2]DESY, Hamburg, Germany
[3]on leave from University Mohammed V in Rabat, Rabat, Morocco

Abstract

The high-brightness electron beam at the Photo Injector Test facility at DESY in Zeuthen (PITZ) is being prepared for dosimetry experiments and radiation biology studies in thin samples. These are the main missions of the FLASH-lab@PITZ, an R&D platform for FLASH and very high energy electron (VHEE) radiation therapy and radiation biology at DESY. These studies require precise information on the electron beam parameters downstream of the exit window, such as the scattering angle and the energy spectrum of the particles as well as the thermal load on the exit window. A Titanium window is compared with a DESY Graphite window design. Heat deposition in the window by a single 22 MeV / 1nC electron bunch of various sizes, its scattering and energy spectrum due to passage through the window are calculated by means of FLUKA Monte Carlo simulations. Time resolved temperature profiles, as induced by the passage of 1ms long electron pulse trains with up to 4500 single pulses, each of them between 0.1 and 60 ps long, were calculated with a self-written finite element method (FEM) code.

INTRODUCTION

Electron beams generated from linear accelerator are used in fundamental nuclear physics, particle physics as well as in applied sciences such as medical applications [1,2]. The Photo-Injector Test Facility at DESY in Zeuthen (PITZ) is starting an R&D project aiming to explore the potential of electron beams in the FLASH dose rate regime for radiation therapy and radiation biology experiments [3]. A wide and unique electron beam parameter range is going to be used for this purpose. An extraction of the electron beam from the vacuum is there-fore needed to irradiate a target placed in air and located at a certain distance from the accelerator exit window. Key parameters of the electron beam, mainly its spot size but also the electron bunch length, the repetition rate and the energy of the electron beam are influencing the heat distribution on the exit window [4,5]. Damages induced by high repetition rate electron beams crossing the exit window might lead to vacuum leaks or in the worst case to a complete collapse of the vacuum/air barrier. In this work, simulations and numerical investigations were carried out in order to estimate the scattering effect on the electron beam crossing an exit window and the resulting heat load under extreme and achievable electron beam parameters at the PITZ facility.

MONTE CARLO SIMULATIONS

Beam Scattering Effect

The interaction of the electron beam with the exit window involves variations of important beam properties, mainly the transverse spatial distribution, the angular distribution and the energy spectrum. For radiation therapy and radiation biology, each of the previous quantities should be precisely identified in the air. In addition, the thermal stability of the exit window should be investigated in order to avoid any vacuum failure or leakage. A FLUKA [6] Monte Carlo model was used to calculate the energy deposition map in the window and its dependence on the electron beam parameters. In this section, we consider two types of exit windows: first one is made of 50 µm thick Titanium, the second one is based on Graphite consisting of a 500 µm carbon fiber reinforced graphite (CF-C, 1.5 g/cm^3) carrier material, coated on one side with less than 50 µm layer of Pyrolytic graphite (PyC, 2 g/cm^3) to make the porous substrate leak tight. Figure 1 shows the distribution of electron scattering angles (left) and energy spectrum (right) at the exit windows generated by a bunch of electrons with an energy of 22 MeV for the Titanium and Graphite window. A Gaussian fit, defines the RMS angle of the electrons at the window exit 17.2 mrad for 50 µm titanium and 20.7 mrad for 550 µm graphite. On the other hand, the analytical estimation of the electron scattering in a thin layer is carried out using the theory of multiple Coulomb scattering. Namely, the Moliere angle is determined as [7]

$$\theta_{RMS} = \frac{13.6MeV}{\beta cp}\sqrt{\frac{x}{X_0}}\left(1 + 0.038 \ln\left(\frac{x}{X_0}\right)\right) \quad (1)$$

where β is the ratio of the electron velocity to the speed of light c, p is the electron momentum, X_0 the radiation length and x is the material. Numerical estimation using Eq. 1 is defined as Moliere angle 16.8 mrad for 50 µm titanium and 21.01 mrad for 550 µm graphite, which is consistent with the simulation results.

The titanium generates less secondary particles and leads to a reduced contribution in the low energy component compared to the Graphite window. The RMS of the angular distribution for the Titanium window is slightly lower with respect to the graphite (Fig. 1).

† zohrab.amirkhanyan@desy.de

ISBN: 978-3-95450-227-1 ISSN: 2673-5490 doi:10.18429/JACoW-IPAC2022-THPOMS010

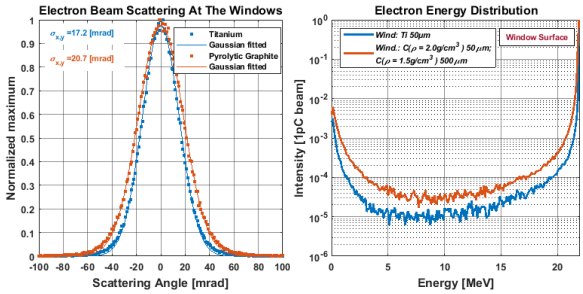

Figure 1: Angular (left) and energy distributions (right) of electrons downstream the exit windows. The blue curves correspond to the 50 µm titanium window and the red ones to the 550 µm thick graphite window.

Energy Deposit and Heat Diffusion in the Exit Window

The electron bunch interaction with a solid material leads to energy loss by different mechanisms [8]: inelastic collisions with orbiting electrons (ionization), inelastic collisions with atomic nuclei (Bremsstrahlung), and elastic collisions with atomic nuclei (Rutherford scattering). As a result of all these processes, in which ionization losses prevail, a thermal energy load arises on the target material. Therefore, it is important to predict the temperature rise and temperature gradients at the exit windows generated by a 1 ms electron pulse train containing up to 4500 single pulses (bunches). To estimate the spatiotemporal distribution of the temperature field induced by electron bunches, two different time ranges processes can be clearly distinguished. The heating phase where the temperature rises continuously quasi instantaneously due to the electron beam interaction with the window material, then followed by the heat diffusion phase where a decay of the hottest temperature regions in the window takes place between two successive bunches and of course after the passage of the whole bunch train.

In this work, we consider only thermal analysis, but to fully understand the operation limits of the exit window, it is also necessary to describe the mechanical stresses caused by temperature gradients.

Heating Phase

The heating is produced due to the interaction of a single electron pulse with the window, and the energy absorbed in a volume element, rapidly turns into a local temperature increase. The heat field distribution for a single bunch passing through the exit window was calculated using FLUKA simulations of the energy deposited in the exit window. The dependence of the energy deposit and the beam size was investigated. Figure 2 shows the heat density deposited by a single electron bunch of 1nC in the titanium (left) or graphite (right) exit window, as a function of the radial distance from the beam centre. Different values of the beam spot sizes in the range of 0.1-1mm were considered.

An electron bunch with a spot size of 0.1mm generates a heat density profile in the exit window with a peak value of $q_{max} = 9.41\,J \cdot cm^{-3}$ for 50 µm titanium and $q_{max} = 4.58\,J \cdot cm^{-3}$ for 550 µm graphite. Obviously, the heat density is inversely proportional to the spot size squared. Starting from energy deposit calculation, the maximum temperature increase could be deduced from the equation $\Delta T = \frac{q_{max}}{\rho c_p}$. At the beam center, the temperature is reaching 3.76 K and 3.29 K for in the Titanium and the Graphite window, respectively. In the above formula, ρ is the mass density and c_p is the specific heat capacity of the material.

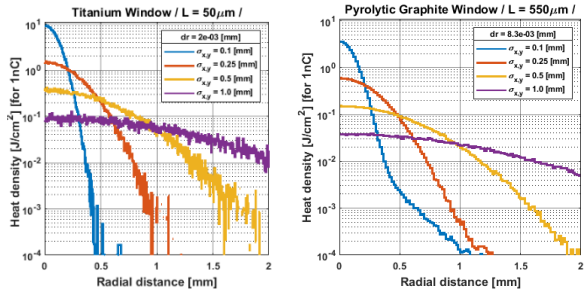

Figure 2: The deposited heat density by a single 1nC electron bunch in a 50 µm thick titanium (left) and a 550 µm thick graphite (right) for different beam spot sizes, as a function of the radial distance from the beam center. The curves correspond to the beam spot sizes 0.1 mm, 0.25 mm, 0.5 mm and 1 mm.

Heat Diffusion Phase

In order to calculate the impact of heat diffusion, the Fourier heat transfer equation had been used with appropriate boundary conditions [9-12]. The heat extraction of the window to the environment occurs due to thermal convection and thermal radiation, which we determined using the boundary conditions at each border of the window. To numerically calculate the thermal evolution of windows, the heat transfer coefficient for convection was set to $5\,W/m^2/K$, and the black graphite and metallic titanium surface emissivity was set to 0.76 and 0.19, respectively. As is known, thermal conductivity, heat capacity, and thermal diffusivity depend on temperature [13-14]. The dependences of heat capacity and thermal conductivity on temperature are shown in Fig. 3.

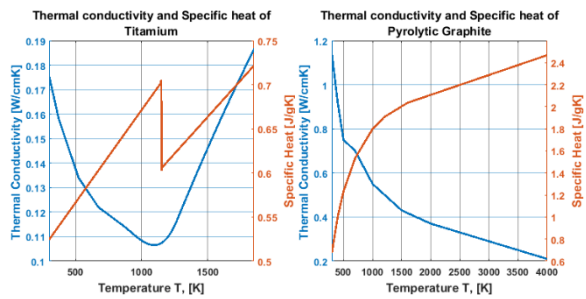

Figure 3: Thermal parameters of titanium (left) and graphite (right) as a function of the temperature in the range $300 - 1850$ K and $300 - 4000$ K respectively. The blue line corresponds to the thermal conductivity, and the red line corresponds to the specific heat.

It is known that the crystal structure of titanium at ambient temperature and pressure is a close-packed hexagonal α phase with a c/a ratio of 1.587. At about 890 °C, the titanium undergoes an allotropic transformation to a body-

ISBN: 978-3-95450-227-1 ISSN: 2673-5490 doi:10.18429/JACoW-IPAC2022-THPOMS010

centred cubic β phase which remains stable to the melting temperature. That means you produce grain boundaries, which make the window very brittle there and will increase in fact the risk of leaks.

Figure 4 shows the temporal variation of temperature at the beam axis for a train with 1000 bunches and 1 nC charge for each, interacting with the titanium (left) resp. graphite (right) window with radius r = 16.5 mm for different beam spot sizes. The calculation of temperature rise based on the FLUKA simulation of the heat density generated in the window and by solving the Fourier heat transfer equation with convection and radiation terms. The temperature dependence of thermal conductivity and heat capacity is included as well.

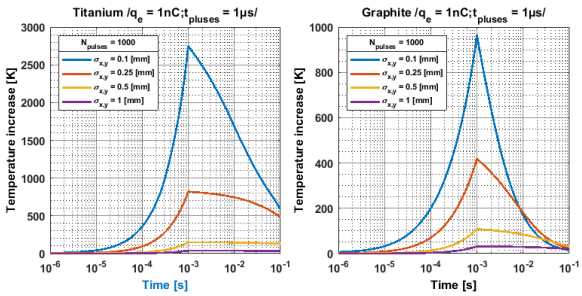

Figure 4: Temporal temperature development on the axis of beam passage and in the middle of the window material, for a train with 1000 bunches with 1 nC charge for each, interacting with the titanium (left) and graphite (right) windows for different beam spot sizes.

The numerical calculation corresponds to the case of a train with $N = 1000$ electron bunches and a total charge of 1000 nC, uniformly distributed over a time interval of 1ms, sequentially crossing and heating the window every 1µs. At such a timescale the i-th bunch hits the target when the heat deposited by the previous (i-1)-th bunch has merely diffused outside the beam spot. Therefore, the heat deposited by the whole train of $N = 1000$ bunches is accumulated and the maximum temperature rise is reached at the beam centre just after the last bunch has penetrated the window at $t = 1$ ms. As an example, the calculated temperature rise at the beam centre is shown for both titanium (Fig. 4 left) and graphite (Fig. 4 right) during a timescale of 0.1 s. The four curves correspond to several beam spot sizes (0.1 mm, 0.25 mm, 5 mm, 1mm). As expected the temperature peak is reached for all curves at the end of the train, after 0.1 ms. Looking at the specific case of beam spot size 0.1mm, the maximum temperature rise (for 1000 bunches) is $\Delta T_{N,Ti} = 2750K$ for the titanium metal (blue curve in Fig. 4 left), and $\Delta T_{N,C} = 965K$ for the graphite material (blue curve in Fig. 4 right). By comparing these values with the analogous ones for a single pulse ($\Delta T_{1,Ti} = 3.76K$ and $\Delta T_{1,C} = 3.29K$), one may note the following points: $\Delta T_N < N \cdot \Delta T_1$; the maximum temperature rise ΔT_N for $N = 1000$ bunches is always lower than $N = 1000$ times the maximum temperature rise for a single pulse ΔT_1. This happens for both titanium and graphite samples due to two cooperative effects: the specific heat increases with temperature causing the nonlinear behaviour between temperature and heat density; the diffusion process provides a temperature peak reduction at a microsecond scale. This means that a small, but non-negligible, fraction of the heat has already diffused out of the heat impact area during the beam passage time.

The thermal dissipation process is not fully completed and a small residual temperature rise remains at 0.1 s . As an example, considering a specific case with a beam spot size of 0.1 mm, the temperature rise for graphite and titanium are $\Delta T_{N,C} = 14.5$ K and $\Delta T_{N,C} = 593$ K.

CONCLUSION

FLASH radiation therapy with electron beams requires tunable electron beam parameters to reach a very high dose rate and a flexible beam size range after crossing the exit window. In this contribution, Monte Carlo simulations and numerical calculations were done in order to estimate the heat distribution for two exit window models: a 50 µm thick, Titanium and a 550 µm carbon rein-forced Graphite type. The calculation has shown that the beam divergence due to the scattering in the Titanium metal is lower compared to the Graphite material. The heating caused by electron bunch train of 1ms length with a round rms-spot size of 0.1 mm and a total charge of 1000 nC, leads to maximal temperatures of 2750 K and 965K for the Titanium and the Graphite respectively. The residual temperature after 0.1 s of the central graphite and titanium windows is still hotter by 14.5 K and 593 K, respectively than the initial temperature.

REFERENCES

[1] R. Mehnert, “Review of industrial applications of electron ac-celerators”, *Nucl. Instrum. Methods Phys. Res., Sect. B*, vol. 113.1-4, pp. 81-87, 1996.

[2] K. Hogstrom, R. Kenneth, and P.R. Almond, "Review of electron beam therapy physics", *Physics in Medicine & Biology,* vol. 51.13, R455, 2006.

[3] F. Stephan, *et al.*, “FLASH-lab@PITZ: New R&D Platform with unique Capabilities for Electron FLASH and VHEE Radiation Therapy and Radiation Biology under Preparation at PITZ”, *Physica Medica: European Journal of Medical Physics,* vol. 94, S36-S37, 2022.

[4] I. Egorov *et al.*, “Self-bearing membrane exit window with the separate anode for sub-microsecond electron accelerator”, *Vacuum,* vol. 173, p109111, 2020.

[5] A. *Knyazeva et al*., “TiN coating effect on the elastoplastic behaviour of Ti film for electron beam exit window", *Vacuum,* vol. 143, pp. 356-362, 2017.

[6] G. *Battistoni et al.,* “The FLUKA code: Description and benchmarking”, *AIP Conference proceedings,* vol. 896, no. 1, American Institute of Physics, 2007.

[7] G. *Lynch*, 0. Dahl, M. Apalak, “Approximations to multiple Coulomb scattering”, *Nucl. Instrum. Methods Phys. Res., Sect. B*, vol. 58, pp. 6-10, 1991. doi:10.1016/0168-583X(91)95671-Y

[8] B. *Rossi*, High Energy Particles, Prentice-Hall, Inc., Englewood Cliffs, NJ, 1952.

ISBN: 978-3-95450-227-1 ISSN: 2673-5490 doi:10.18429/JACoW-IPAC2022-THPOMS010

[9] M. Demirbas, M. Apalak, "Thermal residual stresses analyses of two-dimensional *functionally graded* circular plates with temperature-dependent material properties", *IJERD* vol. 10, pp. 202–213, 2018. doi:10.29137/umagd.444080

[10] H. Kordkheili, G. Amiri, M. Hosseini, "Axisymmetric analysis of a thermoelastic isotropic half-space under buried sources in displacement and temperature potentials", *J. Therm. Stresses*, vol. 40, pp. 237–254, 2017. doi:10.1080/01495739.2016.1234342

[11] A.V. Yasinskii, R.I. Shipka, "Optimization of vertical axisymmetric displacements of a thin circular plate under a nonsta-tionary thermal load", *J. Math. Sci.* vol. 96, pp. 2930–2934, 1999. doi:10.1007/BF02169009.

[12] E. Petronijevic *et al.,* "Resonant absorption in gaas-based nanowires by means of photo-acoustic spectroscopy", *Int. J. Thermophys,* vol. 39, p. 45, 2018. doi:10.1007/s10765-0

[13] J. Valencia, P. Quested, Thermophysical Properties, ASM Handbook, *Volume* 15: *Casting* ASM Handbook Committee, 2008, p 468-481. doi:10.1361/asmhba0005240

[14] P. D. Desai, "Thermodynamic Properties of Titanium", *Int. J. Thermophysics*, vol. 8, no. 6, p. 781, 1987.